HHS Public Access

Author manuscript

Nat Neurosci. Author manuscript; available in PMC 2018 January 17.

Published in final edited form as:

Nat Neurosci. 2017 September ; 20(9): 1213–1216. doi:10.1038/nn.4606.

Gut Microbiota is critical for the induction of chemotherapy-induced pain

Shiqian Shen[1], **Grewo Lim**[1], **Zerong You**[1], **Weihua Ding**[2], **Peigen Huang**[4], **Chongzhao Ran**[3], **Jason Doheny**[1], **Peter Caravan**[3], **Samuel Tate**[1], **Kun Hu**[1], **Hyangin Kim**[1], **Michael McCabe**[1], **Bo Huang**[5], **Zhongcong Xie**[6], **Douglas Kwon**[7], **Lucy Chen**[1], and **Jianren Mao**[1]

[1]MGH Center for Translational Pain Research, Department of Anesthesia, Critical Care and Pain Medicine, Massachusetts General Hospital, Harvard Medical School, Boston, MA 02114

[2]Department of Anesthesia and Pain Medicine, The First Affiliated Hospital, Zhejiang University School of Medicine, Hangzhou, China 310000

[3]MGH/HST Athinoula A. Martinos Center for Biomedical Imaging, Massachusetts General Hospital, Harvard Medical School, Boston, MA 02114

[4]Department of Radiation Oncology, Massachusetts General Hospital and Harvard Medical School, Boston, MA 02114

[5]Basic Sciences Institute, Chinese Academy of Medical Sciences, Beijing, China 100730

[6]Geriatric Anesthesia Research Unit, Department of Anesthesia, Critical Care and Pain Medicine, Massachusetts General Hospital, Harvard Medical School, Boston, MA 02114

[7]Ragon Institute of MGH, MIT, and Harvard, Cambridge, MA 02139, USA; Division of Infectious Diseases, Massachusetts General Hospital and Harvard Medical School, Boston, MA 02114

Abstract

Chemotherapy-induced pain is a dose-limiting condition that affects 30% of patients undergoing chemotherapy. We found that the gut microbiota promotes the development of chemotherapy-induced mechanical hyperalgesia. Oxaliplatin-induced mechnical hyperalgesia was reduced in germ-free mice and in those mice pretreated with antibiotics. Restoration of the microbiota of germ-free mice abrogated this protection. These effects appear to be mediated, in part, by TLR4 expressed on hematopoietic cells, including macrophages.

Chemotherapeutic drugs such as oxaliplatin induce peripheral neuropathy that affects more than 30% of patients under treatment. Chemotherapy-induced peripheral neuropathy (CIPN)

Correspondence should be addressed to S.S. (sshen2@mgh.harvard.edu) or J.M. (jmao@mgh.harvard.edu).

Author contributions: S.S. and J.M. conceived the project and wrote the manuscript. S.S., G.L., Z.Y., W.D., S.T., H.K., and M.M. conducted the experiments. C.R. conducted the bioluminescence study. P.C. carried out the mass spectrometry study. P.H. performed part of the animal study. J.D. contributed to manuscript preparation. K. H. assisted the bone marrow chimera analysis. Z.X. contributed to the TLR4 knockout mice experiment. D. K. contributed to the analysis of gene sequencing data. B.H. and L.C. contributed intellectually to the project.

Competing Financial Interests Statement: The authors have no competing financial interests to report.

often presents with devastating neuropathic pain lasting from months to years, which prevents patients from receiving adequate chemotherapy dosages[1]. Recently, gut microbiota has been shown to play a critical role in the tumor killing effect of many chemotherapeutics drugs, including oxaliplatin[2, 3]. However, it is unknown whether neuropathic pain, a major side effect of chemotherapy, would be influenced by gut microbiota.

We exposed mice with a cocktail of antibiotics in drinking water starting 3 weeks before oxaliplatin administration and continuing throughout the experiment. This treatment regimen reduced the fecal bacterial load by more than two log folds, decreased the α diversity as measured by the Shannon index, and altered the community structure of gut microbiota (Fig 1a–c, Supplementary Fig 1a–c), all of which are consistent with previous reports[4]. We then exposed abx mice (fed with antibiotic water) and H_2O mice (fed with regular water) to either saline or oxaliplatin treatment. While abx mice did not show changes in baseline nociceptive threshold, mechanical hyperalgesia was not detectable after the oxaliplatin therapy (Fig 1d, **$p>0.05$ abx/oxaliplatin *vs.* abx/saline or H_2O/saline) except on day 7 (Fig 1d). In contrast, mechanical hyperalgesia was clearly demonstrated in H_2O mice (Fig 1d, *$p<0.05$ H_2O/oxaliplatin *vs.* H_2O/saline), as shown in previous studies[5, 6]. Thus, temporary gut microbiota eradication protected those mice from developing mechanical hyperalgesia. The same phenomenon was observed in male and female mice, in rats, and in a spontaneous pain behavior test (Supplementary Fig 2a–c). Moreover, we ruled out the possibility that mere exposure to antibiotics directly influences oxaliplatin-induced mechanical hyperalgesia, as intrathecal injection of these antibiotics did not change oxaliplatin-induced mechanical hyperalgesia (Supplementary Fig 2d).

Next, we compared mechanical hyperalgesia in oxaliplatin-treated germ-free (GF) mice and specific pathogen-free (SPF) mice. Mechanical hyperalgesia only developed in SPF mice, but not in GF mice (Fig 1e), indicating that, similar to the effect of gut microbiota eradication in abx mice, the GF status also prevented oxaliplatin-induced mechanical hyperalgesia. Of note, one limitation of the GF mice study was that the behavioral testing period lasted over three weeks, and we cannot completely rule out potential contamination of GF mice during the testing period. To confirm that gut microbiota in SPF mice could mediate oxaliplatin-induced mechanical hyperalgesia, we conventionalized GF mice to SPF status by gastric feeding of feces from SPF mice donors. Conventionalization of GF mice to SPF status abrogated the protection mediated by GF status (Fig 1f), supporting that the gut microbiota in SPF mice likely mediates oxaliplatin-induced mechanical hyperalgesia.

To investigate the underlying mechanism of the above phenotypes, we first examined the possibility that gut microbiota eradication may alter tissue distribution of oxaliplatin. There were no significant differences in platinum concentrations in the spinal cord, dorsal root ganglion (DRG), and serum between abx mice and H_2O mice (Fig 1g, Supplementary Fig 3). Therefore, gut microbiota eradication did not alter the tissue distribution of oxaliplatin. Interestingly, in both groups of mice, the platinum concentrations in DRG were higher than those in the spinal cord and serum (Fig 1g), suggesting that DRG could be a critical site for the pathogenesis of CIPN[7].

In DRG, levels of IL-6 and TNFα and their gene transcripts were lower in abx mice than in H_2O mice after oxaliplatin therapy (Fig 1h and Supplementary Fig 4). These differences were only observed in DRG but not in the spinal cord. However, major immune cell proportions including T cells, B cells, monocytes, dendritic cells, NK cells, and neutrophils in peripheral blood did not differ between abx mice and H_2O mice (Supplementary Fig 5). These results support the notion that DRG is a key anatomical site for the pathogenesis of CIPN[7]. Two additional sets of data suggest that gut microbiota eradication led to dampened inflammatory responses in the DRG following exposure to oxaliplatin. First, consistent with the involvement of reactive oxygen species (ROS) in CIPN[8], we observed that ROS levels in DRG were lower in abx mice than in H_2O mice, using L-012 chemiluminescence as an indicator for ROS[9] (Fig 1i). Second, macrophage infiltration in DRG has recently been identified as a critical event in CIPN[10]. In our experiment, DRG CD11b+ $CD45^{hi}$ cells, presumably macrophages, were less abundant in abx mice than in H_2O mice (Fig 2a, b) after oxaliplatin therapy.

We stimulated mouse primary macrophages with oxaliplatin in the presence or absence of lipopolysaccharides (LPS), a gram negative bacterial wall component. Without LPS, oxaliplatin at 1 μM failed to stimulate macrophages to secrete IL-6 and TNFα, and even at a higher oxaliplatin concentration (10 μM), only a low concentration of IL-6 and TNFα was detected (Fig. 2c). In the presence of LPS, however, oxaliplatin at 1 or 10 μM robustly and dose-dependently stimulated the production of IL-6 and TNFα (Fig 2c). Moreover, we confirmed that the LPS and oxaliplatin concentrations that we used in cell culture did not increase cell death (Supplementary Fig 6). Therefore, oxaliplatin was ineffective in stimulating inflammatory cytokine production *in vitro* without the presence of LPS, indicating that a permissive signal would be required for macrophages to mount an inflammatory response against oxaliplatin.

We posit that this permissive signal is likely to be LPS derived from gut microbiota. To examine this hypothesis, we first measured serum and DRG LPS levels in abx mice and H_2O mice with oxaliplatin or saline treatment. Oxaliplatin treatment increased the serum and DRG LPS levels in both groups of mice when compared with saline treatment. However, the serum and DRG LPS levels were significantly higher in H_2O mice than in abx mice following oxaliplatin treatment (Fig 2d). Next, we examined whether exogenous LPS administration could abrogate the protection of oxaliplatin-induced mechanical hyperalgesia by gut microbiota eradication. Exogenous LPS administration by gastric gavage to abx mice indeed abrogated the protection offered by gut microbiota eradication (Fig 3a). Since LPS is a ligand of Toll-like receptor 4 (TLR4)[11], we compared the development of mechanical hyperalgesia following oxaliplatin treatment in TLR4 knockout ($TLR4^{-/-}$) mice and littermate heterozygous ($TLR4^{+/-}$) mice. Oxaliplatin-induced mechanical hyperalgesia was substantially less severe in $TLR4^{-/-}$mice than in their littermate $TLR4^{+/-}$ counterparts during the entire observation period (Fig 3b), which is in agreement with previous findings on other models of CIPN[12–14]. Taken together, these results suggest that gut microbiota influences the development of mechanical hyperalgesia following oxaliplatin therapy through a LPS-TLR4 pathway.

To determine the contribution of TLR4 expressed on hematopoietic versus non-hematopoietic cells to oxaliplatin-induced mechanical hyperalgesia, we carried out a set of experiments using bone marrow chimeric mice. By using a reciprocal bone marrow transplantation between WT and TLR4$^{-/-}$ mice, we generated bone marrow chimeric mice that only expressed TLR4 on hematopoietic cells versus non-hematopoietic cells (Fig 3c,d). Successful generation of bone marrow chimera was confirmed by the finding that more than 80% and 95% of CD11b^{+} cells in DRG and peripheral blood, respectively, were from the donor origin (Fig 3d, Supplementary Fig 7). We also found that, when hematopoietic cells were from TLR4$^{-/-}$ donors, host mice were protected from oxaliplatin-induced mechanical hyperalgesia regardless of whether their non-hematopoietic cells expressed TLR4 (Fig 3e). These results indicate the TLR4 expressed on hematopoietic cells is responsible for oxaliplatin-induced mechanical hyperalgesia.

We have reported that gut microbiota eradication or GF status prevents the development of mechanical hyperalgesia through its impact on DRG inflammatory responses to oxaliplatin. The exact mechanism underlying this role of gut microbiota remains to be elucidated. Recent studies show that gut microbiota determines the functional maturation of microglia in the central nervous system[15], promotes neutrophils migration in inflammatory responses[16], and, more interestingly, facilitates the migration of monocytes to kidneys following ischemic-reperfusion injury[17]. The present results demonstrate that gut microbiota is indispensable in oxaliplatin-induced mechanical hyperalgesia. LPS has been shown as one of the key factors derived from gut microbiota that determine autoimmunity and inflammation[18]. Our data indicate that LPS enabled and augmented macrophages to secret inflammatory cytokines in response to oxaliplatin exposure, showing a synergy between signals derived from gut microbiota and the impact of oxaliplatin itself on immune cells. This synergy was further supported by the findings that LPS administration abrogated the protective effect offered by gut microbiota eradication (Fig 3a).

Our findings further demonstrate that oxaliplatin is dependent on gut microbiota to exert not only the tumor killing effect[3,19] but also its crucial impact on the development of mechanical hyperalgesia, a major side effect associated with chemotherapy. These findings are not mutually exclusive to previous findings that oxaliplatin has neurotoxicity[7]. In addition, oxaliplatin may directly alter the gut microbiota which contributes to the development of chemotherapy-induced mechanical hyperalgesia. Previously, Amaral et al. found that carrageenan-induced inflammatory pain was attenuated in GF mice, suggesting a key role of gut microbiota in mediating inflammatory pain[20]. Our findings indicate that gut microbiota also plays a key role in mechanical hyperalgesia induced by oxaliplatin. Future studies are needed to examine whether gut microbiota is implicated in other chemotherapy agents-induced mechanical hyperalgesia.

Online Methods

Animals

All procedures and animal use were approved by the Massachusetts General Hospital Institutional Animal Care and Use Committee (IACUC) and were in accordance with the guidelines established by NIH and the International Association for the Study of Pain.

Conventional SPF C56BL/7 mice and Sprague Dawley rats were purchased from the Jackson Laboratory and Charles Rivers Laboratory, respectively. All initial group assignments were randomized. Except for the indicated experiment using female mice, male mice (6–12 weeks of age) were used for the study. For gut microbiota eradication, SPF mice and rats were provided, *ad libitum*, with drinking water containing 0.5 g/L Ampicillin 0.5 g/L Neomycin, 0.5 g/L Metronidazole, and 0.25 g/L Vancomycin (all antibiotics were from Sigma-Aldrich) with 3g/L artificial sweetener Splenda added for three weeks. Antibiotics water was maintained during entire experimental period for chemotherapy-induce pain. When necessary, gastric gavage of oral antibiotics was used. Antibiotics were renewed every other day. For the LPS administration experiment, LPS (Sigma L3012) was administered via gastric gavage at 3 mg/kg on days of oxaliplatin treatment and twice weekly afterwards. Germ-free (GF) mice were obtained from the COX-7 animal facility at the Massachusetts General Hospital. For the fecal transplantation experiment, freshly collected feces from SPF mice were diluted 1:10 with PBS, followed by gastric gavage of 0.3 ml per mouse daily for two consecutive weeks. For intrathecal injection[21]: Antibiotics were prepared in normal saline at the same concentration of oral feeding. Mice were anesthetized with isoflurane anesthesia, and shaved around lumbar spine. A 25μL Hamilton syringe with a 30G needle was inserted between L5–L6 vertebrae and intrathecal access was identified by tail flick. Five μl of antibiotic solution or normal saline was injected. Mice were injected intrathecally every other day starting from three weeks prior to oxaliplatin therapy and continuing through the entire experiment.

Oxaliplatin therapy

To induce mechanical hyperalgesia, oxaliplatin (SAGENT pharmaceuticals, IL) was administered intraperitoneally at 3 mg/Kg for mice and 2 mg/Kg for rats for five consecutive days at a total dose of 15 mg/Kg and 10 mg/Kg, respectively. For *in vitro* culture experiment, oxaliplatin was diluted with DMEM culture medium (Gibco) at indicated concentrations.

Behavioral tests

All behavioral experiments were carried out with the investigators being blinded to treatment conditions. Animals were habituated to the test environment for two consecutive days (30 minutes per day) before baseline testing. Mechanical withdrawal threshold: A von Frey filament was perpendicularly applied to the plantar surface of each hind paw using an up-and-down approach[22, 23]. A threshold force of response (in grams) was defined as the first filament that evoked at least two withdrawals out of five applications. Seven or fewer filaments were applied to animals. Facial grooming is evaluated by counting the number of forepaw rubbing and hindpaw scratching for 10 minutes[24]. GF animal testing was performed in a facility room with HEPA air filter and a testing hood with laminar flow. Test performers wore sterile gown and gloves. Testing enclosures were autoclaved prior to use. Of note, the GF behavioral testing period was over three weeks. We could not completely rule out potential contamination occurred during the testing period despite surveillance Q-PCR was negative[25].

Real-time PCR for cytokine genes

cDNA was prepared from 1000 ng of total RNA according to the protocol for SuperScript IV Reverse transcription (Invitrogen, Grand Island, NY). For each sample, real-time quantitative RT-PCR was then performed using the Taqman (Thermo-Fisher) probes for *Tnf-a*, *Il-6*, and *Gapdh* with Universal PCR Master Mix (Applied Biosystems) under the cycling conditions required in the protocol for the Universal PCR Master Mix protocol. The expression of candidate genes in each group of samples was normalized to *Gapdh* to obtain a ΔCt value and to calculate a 2^-(mean ΔΔCt).

ELISA

Levels of IL-6 and TNFα were measured by ELISA (R& D Biosystems, Minneapolis, MN)) according to the manufacturer's instructions. The lower detection limit was 1.8 pg/ml for Il-6 and 7.2 pg/mL for TNFα. The assay plates were read at 450 nm and 540 nm. All samples were run in duplicates.

LPS (endotoxin) assay

All materials used for both sample preparation and testing were pyrogen free. LPS concentrations in plasma and tissue homogenate were measured by an endotoxin assay based on a limulus amebocyte extract with a chromogenic limulus amebocyte lysate (LAL) assay (Pierce™ LAL Chromogenic Endotoxin Quantitation Kit). Samples were diluted in pyrogen-free water and heated to 70°C for 10 min to inactivate inhibitors agents that interfere with the assay. All samples were tested in triplicate, and results were accepted when the intra-assay coefficient of variation was 15%. The endotoxin content was expressed as endotoxin units per milliliter (EU/mL) or endotoxin units per 100mg of tissue.

DNA extraction and quantification of fecal bacteria

Fecal DNA was extracted with DNA Stool Kit (MoBio) according to the manufacturer's instruction. The abundance of eubacteria in feces was measured by qPCR using a StepOnePlus instrument (Applied Biosystems) with the fecal DNA and 16s rRNA gene primers for eubacteria. The sequences of the primers are ACT CCT ACG GGA GGC AGC AGT (UniF 340) and ATT ACC GCGGCT GGC (UniR 514). The real-time PCR program started with an initial step at 95°C for 10 min, followed by 40 cycles of 95°C 30 s and 60°C 1 min. The real-time PCR was done using SYBR green Mastermix (Qiagen). Bacterial numbers was determined using standard curves constructed with DNA of E. Coli strain DH10α as reference bacteria. 16s rRNA gene sequencing and data analysis were performed by BGI America (Cambridge, MA). Briefly, after amplicon based sequencing, OTUs were clustered using USEARCH (7.0.1090) with a 97% threshold. Greengene V201305 was used as reference database for taxonomic analysis. MixOmics of Software R was used for PLS-DA analysis.OTU rank curse was generated by software R (V3.1.1).The tag number of each taxonomic rank (Phylum, Class, Order, Family, Genus, Species) or OTU in different samples were summarized in histogram generated by software R (V3.1.1)[2,3,4,18]. Sequencing data are available through NCBI BioProject number PRJNA388399.

Bioluminescence assay

Three days after oxaliplatin injection, mice were injected with luminescent probe L-012 (Wako, Richmond, VA) at 100mg/Kg. Within three to five minutes after injection, rats were sacrificed and (lumbar) L3-5 DRGs were obtained for IVIS Spectrum (Xenogen, Alameda, CA) study. L-012 shows luminescence after chemical reaction with ROS. To calculate bioluminescence, radiance (photons/s/cm^2/sr) was obtained within 15 minutes after L-012 injection.

Platinum concentration by inductively coupled plasma mass spectrometry (ICP-MS) analysis

Tissue sample was transferred to a glass sample vial. The sample weight was recorded. The sample was then digested with 1.5% HNO3: 4% HCl to 20 mL volume at 37 °C overnight. Elemental Analysis was completed using ICP-MS (Agilent Technologies, 8800 ICP-MS-QQQ). Calibration samples were prepared from a serial dilution of a 1 μg/g and 10 ng/g Pt (NIST SRM 3140) solution. Briefly, 10, 25, 50, 75, 100, 150, 200 pg/g standards were prepared by diluting 0.100, 0.250, 0.500, 0.750, 1.00,1.50, and 2 mL of a 1 ng/g Pt solution and was transferred to a 18 mL LDPE sample vial. The standards were diluted to a total of 10 mL using 1.5% HNO3: 4% HCl solution, respectively. The weight of the empty vial, the vial containing sample, and the vial containing the final dilution was recorded. The exact concentration in each standard was determined by difference. The three analyzed elements included Platinum (Pt, analyte), Lutetium (Lu, internal standard), and Dysprosium (Dy, internal standard). Samples were run in triplicate, with each one or the triplicate consisting of 10 measurement repetitions. A calibration curve was constructed from the external calibration samples. The limit of detection (LOD) for the sample run was 0.48pg/g. The limit of quantitation (LOQ) was also determined using the formula above with k =10. The LOQ for the ICP-MS run was 1.6pg/g.

Flow cytometry

For DRG staining, mice were anesthetized by isoflurane anesthesia followed by perfusion through left ventricle cannulation with a 20G needle. For each mouse, 20 ml of ice-cold normal saline was perfused to minimize blood contamination in the sample. Six DRG samples were obtained from each mouse. DRG samples were minced and digested with Liberase TL (Roche) at 37 °C for 60 minutes in RPMI-1640 medium with intermittent vortex. The samples were then filtered through a nylon membrane with 60μm pore size, followed by centrifugation. A Percoll (Sigma) gradient (70%–40%) was used for cell isolation. For peripheral blood staining, 20 μl of peripheral blood obtained from retro-orbital veins was used. For cultured macrophage staining: macrophages cultured in RPMI-1640 were washed to PBS three times, followed by a brief trypsin treatment to detach cells from culture plate. Flow cytometry staining was performed in room temperature for 10 minutes except for Annexin V and 7-AAD staining. Antibodies (anti-CD3 catalog #100235;-CD4 catalog #100413; -CD11b catalog #101222; -CD335 catalog #137617;-CD11c catalog #117309;-Ly-6G catalog #127623, AnnexinV catalog #640905; 7-AAD catalog #420403) were obtained from BioLegend. For Annexin V and 7-AAD staining: a binding buffers containing 140 mM NaCl, 4 mM KCl, 0.75 mM $MgCl_2$, 2.5mM $CaCl_2$ and 10 mM HEPES

in DDW was used at 0.2 ml per sample. Annexin V and 7-AAD were added to the sample 10 min prior to acquisition by flow cytometer. All samples were acquired by LSR II (BD) flow cytometer. Data were analyzed with Flowjo (FlowJo) software.

Macrophage isolation and culture[26]

Mice were euthanized and soaked in 70% ethanol. Ten ml of cold PBS was injected to peritoneal cavity followed by needle aspiration. Aspirated fluid was centrifuged and cells (including neutrophils and macrophages) were resuspended in DMEM medium. A total of 4×10^5cells/well was added to a 24-well plate. The cells were allowed to adhere to culture plate for 2 hours at 37°C. Non-adherent cells were removed by gently washing three times with warm PBS. Adherent cells were macrophages and were used for subsequent culture in the presence of LPS and oxaliplatin at desired concentrations.

Statistical analysis and sample size

No statistical methods were used to pre-determine sample sizes but our sample sizes are similar to those reported in previous publications[27]. Data distribution was assumed to be normal but this was not formally tested. Behavioral data were analyzed using two-way analysis of variance (ANOVA) repeated across time points and groups. One-way ANOVA was used to analyze the data from various assays (qPCR, ELISA). Post-hoc Waller-Duncan K-ratio t test (two-tailed) was performed to determine the source(s) of differences. SPSS 12.0 software was used for the statistical analyses. All data were expressed as mean ± SEM and the statistically significant level was set at $P<0.05$.

Data Availability

The data that support the findings of this study are available from the corresponding author upon reasonable request.

Supplementary Material

Refer to Web version on PubMed Central for supplementary material.

Acknowledgments

S. Shen received support from NIH grant 5T32GM007592, Foundation of Anesthesia Research and Education grant, and departmental research fund. This work was supported by NIH grant R01DE022901 (J.M). W. Ding was supported by Hangzhou Science and Technology Plan No. 20130633B02 and Zhejiang Medical Science and Technology Plan No. 2011KYB064. The ICP-MS equipment was purchased with support from NIH grant S10OD010650. We thank P. Waghorn and O. Pinkhasov for assistance with ICP-MS study; MGH COX-7 animal facility and CNY149 animal facility for animal husbandry; L. Chen for genomic data analysis; Z. Zhang and J. Moon for bone marrow transplantation; Y. Dong and J. Lan for their assistance with TLR4 knockout animals; Q. Chen for critical comments on the manuscript.

References

1. Hershman DL, et al. Prevention and management of chemotherapy-induced peripheral neuropathy in survivors of adult cancers: American Society of Clinical Oncology clinical practice guideline. J Clin Oncol. 2014; 32:1941–1967. [PubMed: 24733808]
2. Viaud S, et al. The intestinal microbiota modulates the anticancer immune effects of cyclophosphamide. Science. 2013; 342:971–976. [PubMed: 24264990]

3. Iida N, et al. Commensal bacteria control cancer response to therapy by modulating the tumor microenvironment. Science. 2013; 342:967–970. [PubMed: 24264989]
4. Hill DA, et al. Commensal bacteria-derived signals regulate basophil hematopoiesis and allergic inflammation. Nat Med. 2012; 18:538–546. [PubMed: 22447074]
5. Xiao WH, Bennett GJ. Effects of mitochondrial poisons on the neuropathic pain produced by the chemotherapeutic agents, paclitaxel and oxaliplatin. Pain. 2012; 153:704–709. [PubMed: 22244441]
6. Renn CL, et al. Multimodal assessment of painful peripheral neuropathy induced by chronic oxaliplatin-based chemotherapy in mice. Molecular pain. 2011; 7:29. [PubMed: 21521528]
7. Sprowl JA, et al. Oxaliplatin-induced neurotoxicity is dependent on the organic cation transporter OCT2. Proceedings of the National Academy of Sciences of the United States of America. 2013; 110:11199–11204. [PubMed: 23776246]
8. Barriere DA, et al. Paclitaxel therapy potentiates cold hyperalgesia in streptozotocin-induced diabetic rats through enhanced mitochondrial reactive oxygen species production and TRPA1 sensitization. Pain. 2012; 153:553–561. [PubMed: 22177224]
9. Kielland A, et al. In vivo imaging of reactive oxygen and nitrogen species in inflammation using the luminescent probe L-012. Free Radic Biol Med. 2009; 47:760–766. [PubMed: 19539751]
10. Zhang H, et al. Dorsal Root Ganglion Infiltration by Macrophages Contributes to Paclitaxel Chemotherapy-Induced Peripheral Neuropathy. The journal of pain: official journal of the American Pain Society. 2016; 17:775–786. [PubMed: 26979998]
11. Poltorak A, et al. Defective LPS signaling in C3H/HeJ and C57BL/10ScCr mice: mutations in Tlr4 gene. Science. 1998; 282:2085–2088. [PubMed: 9851930]
12. Wardill HR, et al. Irinotecan-Induced Gastrointestinal Dysfunction and Pain Are Mediated by Common TLR4-Dependent Mechanisms. Molecular cancer therapeutics. 2016; 15:1376–1386. [PubMed: 27197307]
13. Li Y, et al. The Cancer Chemotherapeutic Paclitaxel Increases Human and Rodent Sensory Neuron Responses to TRPV1 by Activation of TLR4. The Journal of neuroscience: the official journal of the Society for Neuroscience. 2015; 35:13487–13500. [PubMed: 26424893]
14. Li Y, et al. Toll-like receptor 4 signaling contributes to Paclitaxel-induced peripheral neuropathy. The journal of pain: official journal of the American Pain Society. 2014; 15:712–725. [PubMed: 24755282]
15. Erny D, et al. Host microbiota constantly control maturation and function of microglia in the CNS. Nature neuroscience. 2015; 18:965–977. [PubMed: 26030851]
16. Karmarkar D, Rock KL. Microbiota signalling through MyD88 is necessary for a systemic neutrophilic inflammatory response. Immunology. 2013; 140:483–492. [PubMed: 23909393]
17. Emal D, et al. Depletion of Gut Microbiota Protects against Renal Ischemia-Reperfusion Injury. Journal of the American Society of Nephrology: JASN. 2016
18. Vatanen T, et al. Variation in Microbiome LPS Immunogenicity Contributes to Autoimmunity in Humans. Cell. 2016; 165:1551. [PubMed: 27259157]
19. Yang J, et al. Cells deficient in the base excision repair protein, DNA polymerase beta, are hypersensitive to oxaliplatin chemotherapy. Oncogene. 2010; 29:463–468. [PubMed: 19838217]
20. Amaral FA, et al. Commensal microbiota is fundamental for the development of inflammatory pain. Proceedings of the National Academy of Sciences of the United States of America. 2008; 105:2193–2197. [PubMed: 18268332]
21. Njoo C, Heinl C, Kuner R. In vivo SiRNA transfection and gene knockdown in spinal cord via rapid noninvasive lumbar intrathecal injections in mice. Journal of visualized experiments: JoVE. 2014
22. Bennett GJ, Xie YK. A peripheral mononeuropathy in rat that produces disorders of pain sensation like those seen in man. Pain. 1988; 33:87–107. [PubMed: 2837713]
23. Tal M, Bennett GJ. Extra-territorial pain in rats with a peripheral mononeuropathy: mechano-hyperalgesia and mechano-allodynia in the territory of an uninjured nerve. Pain. 1994; 57:375–382. [PubMed: 7936715]
24. Romero-Reyes M, et al. Spontaneous behavioral responses in the orofacial region: a model of trigeminal pain in mouse. Headache. 2013; 53:137–151. [PubMed: 22830495]

25. Fontaine CA, et al. How free of germs is germ-free? Detection of bacterial contamination in a germ free mouse unit. Gut microbes. 2015; 6:225–233. [PubMed: 26018301]

26. Zhang X, Goncalves R, Mosser DM. The isolation and characterization of murine macrophages. Current protocols in immunology. 2008 Chapter 14 Unit 14 11.

27. Kim H, et al. Brain indoleamine 2,3-dioxygenase contributes to the comorbidity of pain and depression. The Journal of clinical investigation. 2012; 122:2940–2954. [PubMed: 22751107]

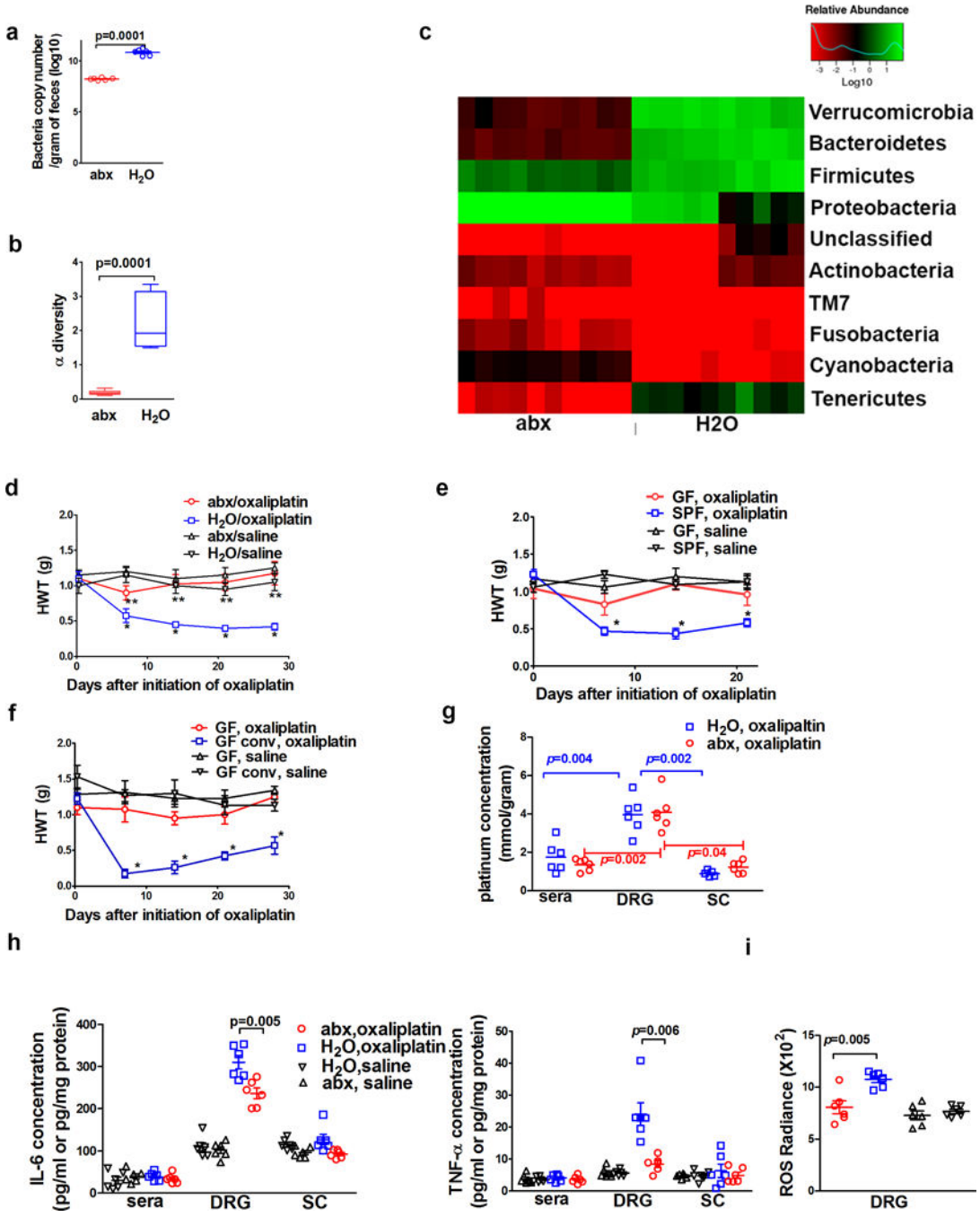

Fig 1. Temporary eradication of gut microbiota prevents oxaliplatin-induced mechanical hyperalgesia

a–c) Impacts of antibiotic water feeding on mice gut microbiota. Fecal samples were obtained after three weeks of antibiotic water (abx, N=10) or regular water (H_2O, N=10) followed by DNA isolation from these samples. **a**) Antibiotics feeding reduced bacterial load as determined by semi-quantitative real-time PCR. **b**) Antibiotics feeding reduced the α diversity of microbiota. **c**) Antibiotics feeding altered bacterial community structure as shown in the phylum analysis. **d**) Gut microbiota eradication prevented the development of

oxaliplatin-induced mechanical hyperalgesia. Mice were fed on antibiotics water (abx) or regular water (H_2O) prior to oxaliplatin or saline treatment (as control). Hindpaw mechanical withdrawal threshold (HWT) was examined at indicated time points after oxaliplatin therapy. N=6 each group. * $p<0.05$ H_2O/oxaliplatin *vs.* abx/oxaliplatin. **p>0.05 abx/oxaliplatin vs. abx/saline or H2O/saline. **e**) Germ-free (GF) status protected mice from oxaliplatin-induced mechanical hyperalgesia. GF or specific pathogen free (SPF) mice were given oxaliplatin or saline. HWT was examined at indicated time points after oxaliplatin therapy. * $p<0.05$ SPF, oxaliplatin *vs.* all other groups. N=7 each group. **f**) GF conventionalization abrogated the protection of mechanical hyperalgesia offered by GF status. To conventionalize GF mice, feces from SPF mice were diluted with PBS and administered daily via gastric gavage for three weeks. GF and conventionalized GF (GF conv) mice were treated with oxaliplatin or saline. Conventionalization of GF mice abrogated the protection offered by GF status. * $p<0.05$ GF conv, oxaliplatin *vs.* GF, oxaliplatin. N=8 for GF, oxaliplatin; N=7 for GF, saline; N=7 for GF conv, oxaliplatin; N=6 for GF conv, saline. **g**) Gut microbiota eradication did not change tissue oxaliplatin distribution (N=6 each group). Spinal cord (sc), serum and dorsal root ganglion (DRG) concentrations of platinum were determined by ICP-MS. Two-way ANOVA test suggested abx treatment did not change tissue platinum distribution ($p=0.42$) while types of tissues have significant influence on platinum levels ($p=0.001$). Post-hoc t-tests (p values in the figure). were performed to identify the impact of tissue type on platinum levels **h**) DRG cytokine levels for IL-6 and TNF-α were lower in mice with eradicated gut microbiota than those in mice with normal gut microbiota (N=6 each group, one-way ANOVA indicated there was significant difference in DRG samples, and subsequent post-hoc t-test was used to determine the difference between the abx and H_2O groups). Sera and spinal cord levels for IL-6 and TNF-α were not significantly different among groups (N=6 each group, one-way ANOVA test for sera IL-6 samples, $p=0.58$; spinal cord IL-6 samples, $p=0.06$; sera TNF-α samples, $p=0.88$; spinal cord TNF-α samples, $p=0.75$). **i**) Reduced levels of reactive oxygen species (ROS) in DRG from mice with eradicated gut microbiota. At day 10 after the initiation of oxaliplatin therapy, levels of ROS were determined with IVIS using L-012 as a chemiluminescent probe. N=6 each group. One-way ANOVA test followed by post-hoc test were used for statistical analysis.

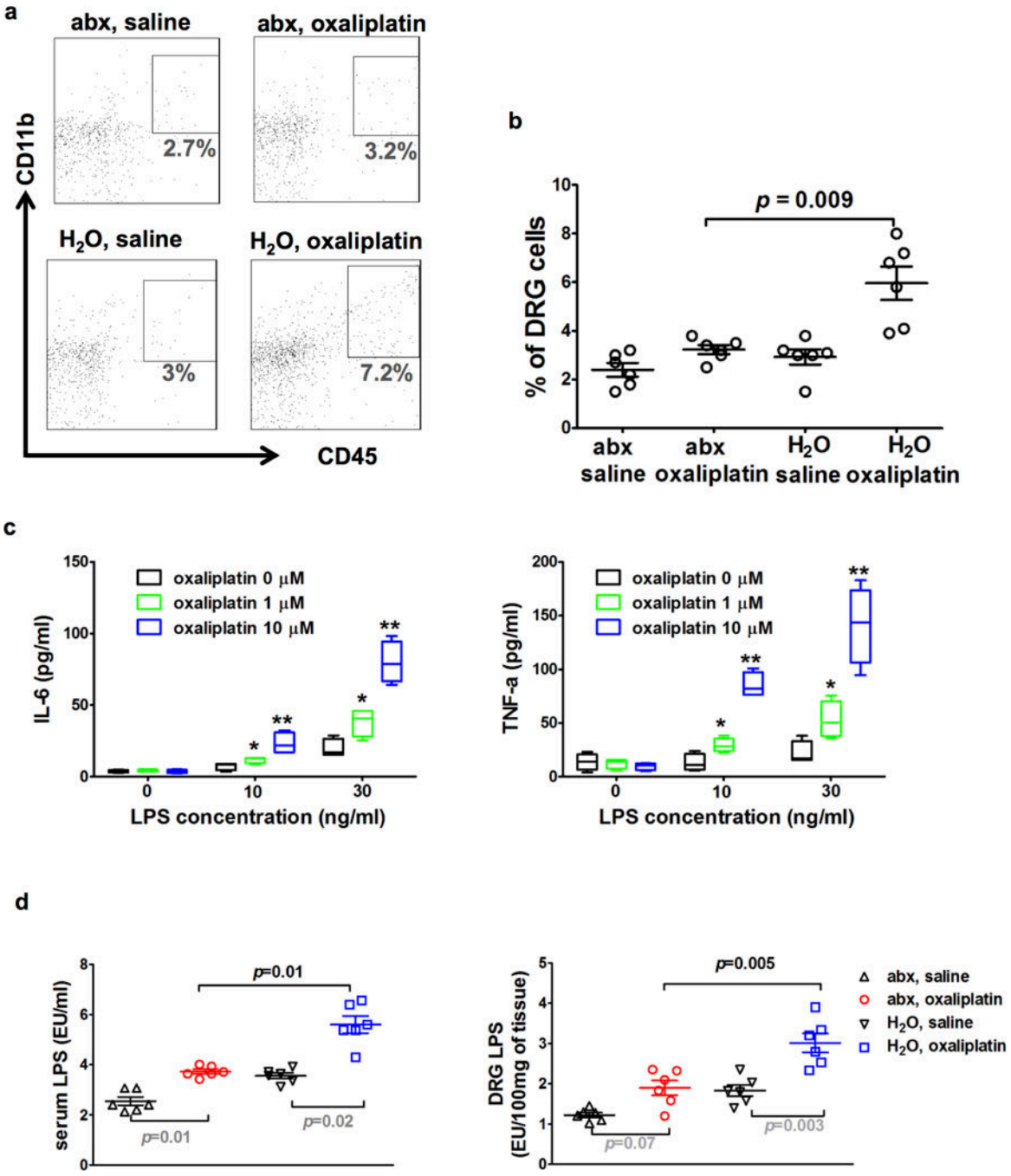

Fig 2. Gut microbiota is critical for DRG inflammatory responses

a–b) DRG flow cytometry staining for macrophages. Mice were fed on antibiotics water (abx) or regular water (H_2O) prior to oxaliplatin or saline treatment. Ten days after the initiation of oxaliplatin or saline treatment, DRG samples were collected and processed for flow cytometry staining. Dot plots in **a**) are representative stainings for macrophages ($CD11b+CD45^{hi}$ cells) of each group. Percentages of macrophages in DRG cells were plotted in **b**). Percentages of macrophages were significantly higher in the 'H_2O, oxaliplatin' group than in the 'abx, oxaliplatin' group (N=6 each group, p=0.0001 by one-way ANOVA,

post-hoc t-test p=0.009). **c**) A permissive effect of LPS on production of IL-6 and TNF-α in macrophages. Macrophages were collected from peritoneal cavity for culture in the presence of LPS and oxaliplatin at indicated concentrations. IL-6 and TNF-α levels in culture supernatant were determined at 24 hours after oxaliplatin and LPS stimulation with ELISA. * and ** indicate post-hoc t-test performed after one-way ANOVA test suggesting significant differences exist among three groups at given LPS concentration. *$p<0.05$ vs oxaliplatin 0, ** $p<0.05$ vs oxaliplatin 1μM. Data represent quadruplicate wells, mean +/− SEM. **d**) LPS (endotoxin) levels in serum and DRG. Mice were fed on antibiotics water (abx) or regular water (H_2O) prior to oxaliplatin treatment or saline treatment as control. Ten days after the initiation of oxaliplatin or saline treatment, serum and DRG samples were collected and processed for endotoxin assay. LPS levels in sera and DRG were higher in the 'H_2O, oxaliplatin' group than in the 'abx, oxaliplatin' group. Post-hoc t-tests (*p* values) were performed after one-way ANOVA tests indicating significant difference present among all groups (N=6 each group).

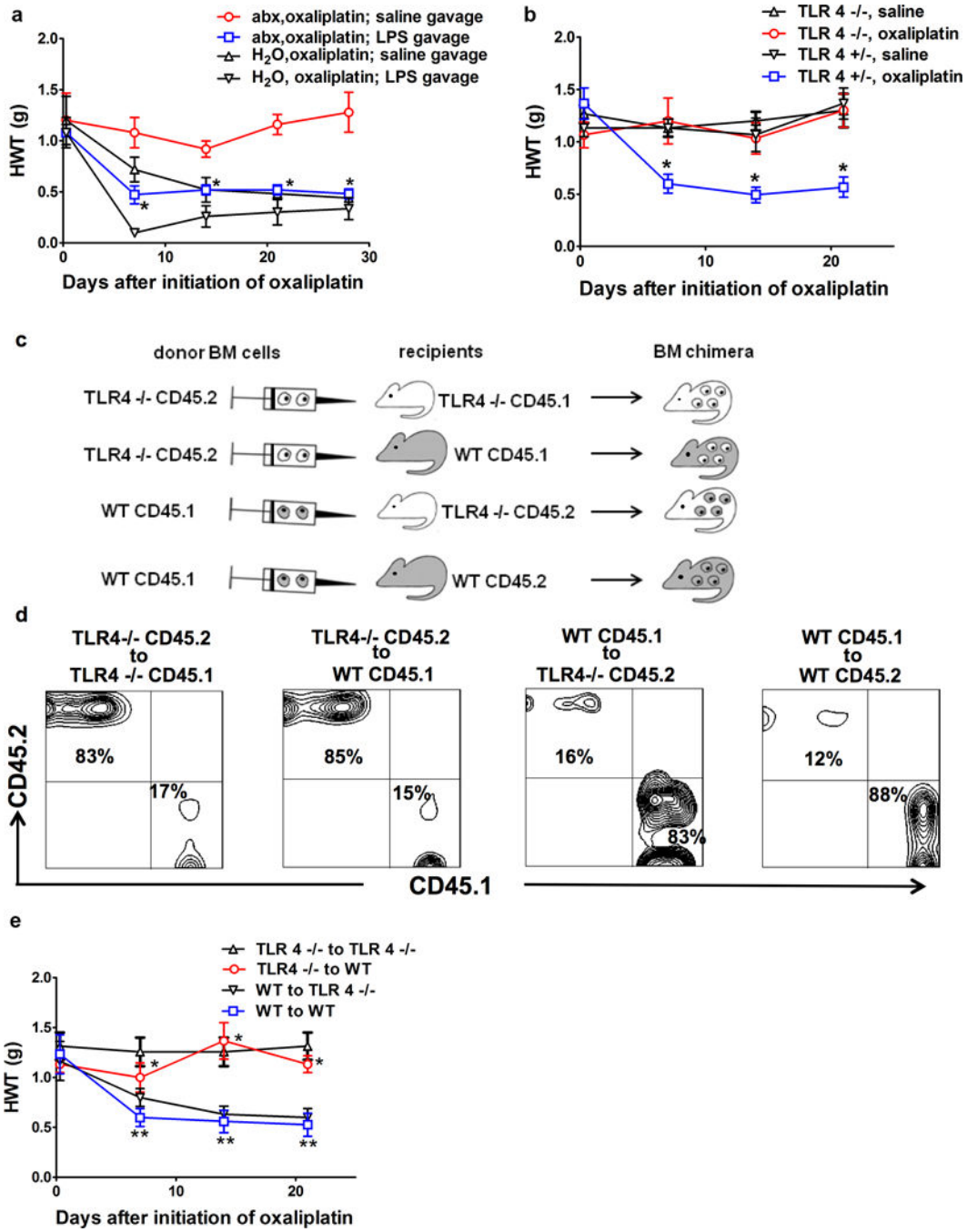

Fig 3. TLR4 on hematopoietic cells is critical for oxaliplatin-induced mechanical hyperalgesia

a) Exogenous administration of LPS through gastric gavage reversed the effect of gut microbiota eradication. Mice were fed with antibiotic water (abx) or regular water (H_2O), followed by oxaliplatin injection. LPS (3mg/Kg) or normal saline was administered on days of oxaliplatin injection and twice weekly afterwards. *p<0.05, abx,oxaliplatin; LPS gavage *vs.* abx, oxaliplatin; saline gavage, N=7 each group. **b**) Toll-like receptor 4 (TLR4) knockout mice did not develop oxaliplatin-induced mechanical hyperalgesia. TLR4 knockout ($TLR4^{-/-}$) or littermate heterozygous ($TLR\ 4^{+/-}$) mice were treated with oxaliplatin or saline

and were examined at indicated time points for hindpaw mechanical withdrawal threshold (HWT) (N=6 each group). * $p<0.05$ WT, oxaliplatin *vs.* all other groups. **c–d**) Generation of bone marrow (BM) chimeras. **c**) Flow chart for BM chimeric mice generation. Recipients were irradiated 500 Rad × 2 followed by bone marrow cells injection. Donor bone marrow cells were derived from TLR4$^{-/-}$ or WT mice, and were injected to WT or TLR4$^{-/-}$ recipients, using a cross-over study design. CD 45.1 and CD45.2 congenic markers were used to distinguish between donor-derived and recipient-derived hematopoietic cells. **d**) Confirmation of successful generation of bone marrow chimera. Fourteen weeks after BM transplantation, DRG samples were collected and stained for CD45.1 and CD45.2 congenic markers. Contour plots were gated on CD11b^{+} and CD3^{-} cells. Each panel represents 6 independent stainings. **e**) TLR4 on hematopoietic cells is critical for oxaliplatin-induced mechanical hyperalgesia. BM chimeric mice generated as shown in **c–d**) were treated with oxaliplatin (N=6 each group). In TLR4$^{-/-}$ to WT group, hematopoietic cells were from TLR4$^{-/-}$ donors. These mice were protected from oxaliplatin-induced mechanical hyperalgesia despite the presence of TLR4 on host-derived radio-resistant cells. *$p<0.05$ TLR4$^{-/-}$ to WT *vs.* WT to WT. In contrast, in WT to TLR4$^{-/-}$ group, hematopoietic cells were from WT donors, these mice developed oxaliplatin-induced mechanical hyperalgesia despite the absence of TLR4 on host-derived radio-resistant cells. ** $p> 0.05$ WT to TLR4$^{-/-}$ *vs.* WT to WT.